crystals

MDPI

Supplementary Materials

Fe_2O_3 Nanoparticles Deposited over Self-Floating Facial Sponge for Facile Interfacial Seawater Solar Desalination

Yuzheng Lu [1], Naila Arshad [2], Muhammad Sultan Irshad [3,*], Iftikhar Ahmed [4,*], Shafiq Ahmad [5], Lina Abdullah Alshahrani [6], Muhammad Yousaf [7], Abdelaty Edrees Sayed [5] and Muhammad Nauman [8]

Note S1. Characterization

The chemical composition of Fe_2O_3 NPs nanoparticles was investigated through X-ray photoelectron spectroscopy (XPS) was operated on a Thermo Fisher Scientific Escalab 250Xi (Thermo Fisher Scientific Inc., Waltham, Massachusetts. Field emission scanning electron microscopy (FESEM, JSM7100F, Japan) was utilized to analyze the surface morphology of bare facial sponge, Fe_2O_3/facial sponge, and in-situ polymerized Fe_2O_3/facial sponge (Fe_2O_3@PPy). The UV- vis- NIR spectrophotometer (Shimadzu Corp., Tokyo, Japan, computed by employing an integrated sphere) was operated to determine the absorption spectrum of synthesized samples by considering BaSO4 as reference. The optical microscope (Olympus IX71, Japan) was performed to evaluate the oil-in-water emulsion and distilled water morphology. The contact angle test of bare facial sponge and Fe_2O_3@PPy solar evaporator surface was examined using contact angle meter, Dongguan Precise Testing Machine Co., Ltd.

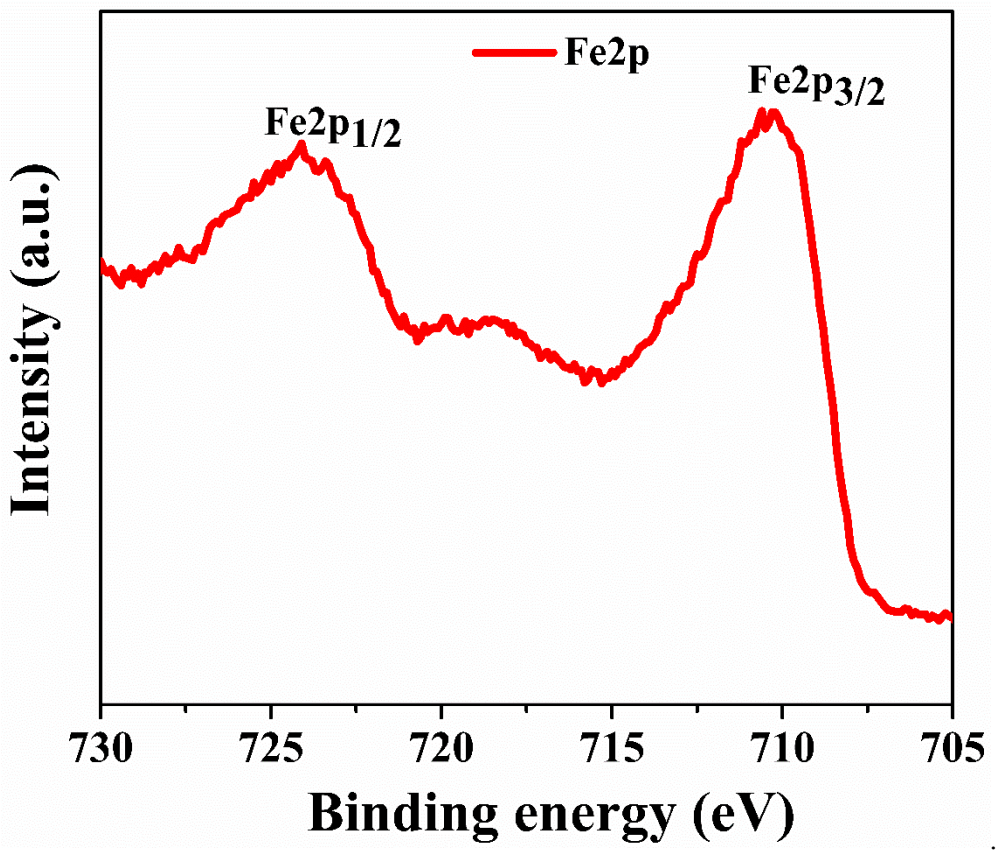


Figure S1. Fe 2p scan of Fe_2O_3 NPs.

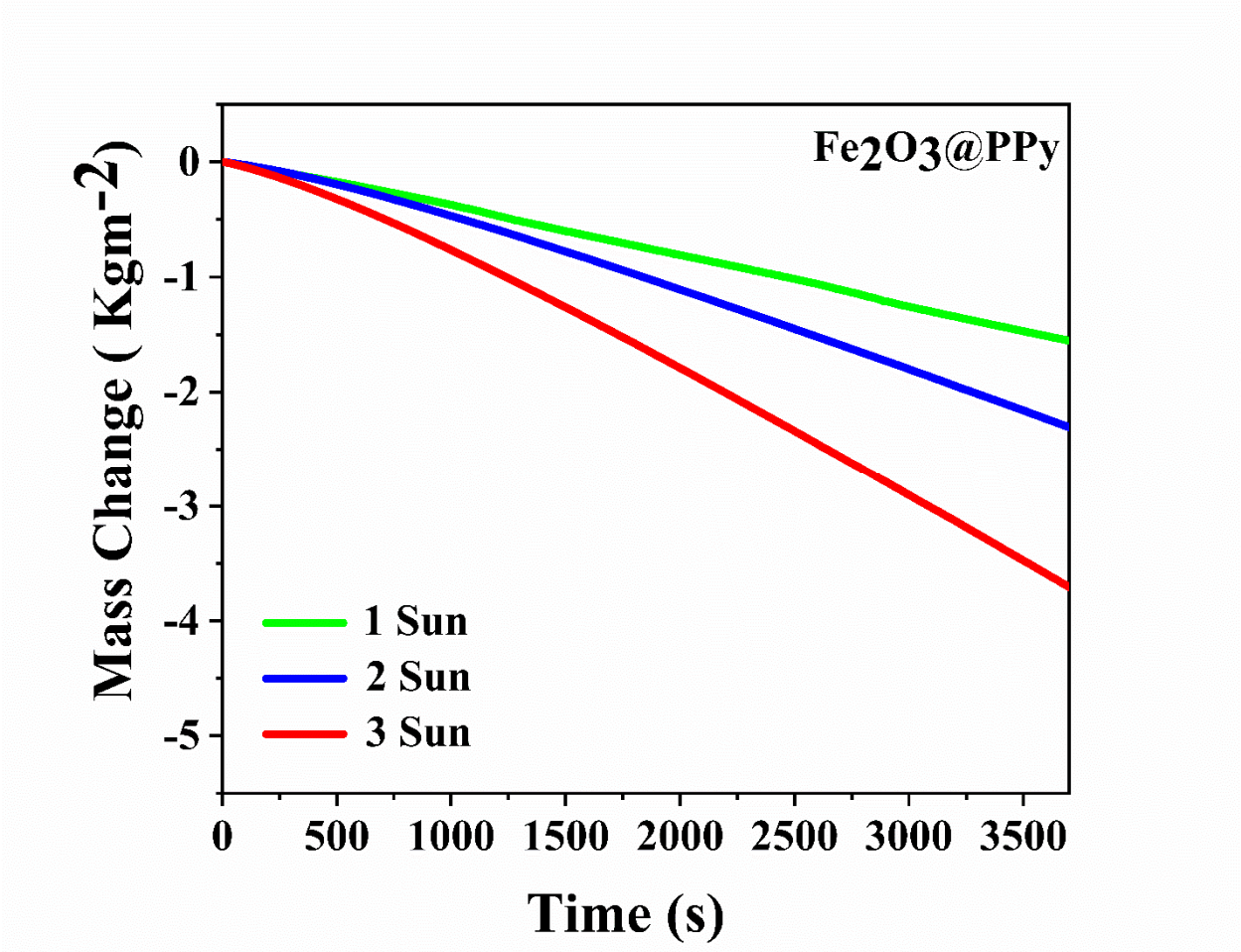


Figure S2. Time dependent mass change under different solar intensities.

Table S1. Detailed performance comparison with the recent successful solar evaporators.

Sr. No	Solar Driven System	Absorption (%)	Evaporation Rate (Kg $m^{-2}h^{-1}$)	Efficiency (%)	Ref.
1.	Wood/PPy	99	1.014	72.5	[1]
2.	PPy-NF-PUS	93	1.256	82.18	[2]
3.	HN/NiO	92.1	1.37	85.8	[3]
4.	Carbon foam	96.19	1.57	86	[4]
5.	Graphene membrane	99.9	1.37	90	[5]
6.	rGO/Ni Foam	89	1.33	83.4	[6]
7.	rGo/Cotton	95	1.47	NA	[7]
8.	Black sand	98.25	1.43	81	[8]
9.	PPy/Wood	97.5	1.33	83	[9]
10.	Fe_2O_3@PPy	94	1.52	95	This work

Reference:

1. C. Wang, J. Wang, Z. Li, K. Xu, T. Lei, W. Wang, Superhydrophilic porous carbon foam as a self-desalting monolithic solar steam generation device with high energy efficiency, J. Mater. Chem. A. 8 (2020) 9528–9535.
2. S. Wang, Y. Fan, F. Wang, Y. Su, X. Zhou, Z. Zhu, H. Sun, W. Liang, A. Li, Potentially scalable fabrication of salt-rejection evaporator based on electrogenerated polypyrrole-coated nickel foam for efficient solar steam generation, Desalination. 505 (2021) 114982. https://doi.org/https://doi.org/10.1016/j.desal.2021.114982.

3. D.-D. Qin, Y.-J. Zhu, R.-L. Yang, Z.-C. Xiong, A salt-resistant Janus evaporator assembled from ultralong hydroxyapatite nanowires and nickel oxide for efficient and recyclable solar desalination, Nanoscale. 12 (2020) 6717–6728.
4. Z. Wang, Y. Yan, X. Shen, C. Jin, Q. Sun, H. Li, A wood--polypyrrole composite as a photothermal conversion device for solar evaporation enhancement, J. Mater. Chem. A. 7 (2019) 20706–20712.
5. C. Li, D. Jiang, B. Huo, M. Ding, C. Huang, D. Jia, H. Li, C.-Y. Liu, J. Liu, Scalable and robust bilayer polymer foams for highly efficient and stable solar desalination, Nano Energy. 60 (2019) 841–849.
6. X. Shan, Y. Lin, A. Zhao, Y. Di, Y. Hu, Y. Guo, Z. Gan, Porous reduced graphene oxide/nickel foam for highly efficient solar steam generation, Nanotechnology. 30 (2019) 425403.
7. Q. Zhang, H. Yang, X. Xiao, H. Wang, L. Yan, Z. Shi, Y. Chen, W. Xu, X. Wang, A new self-desalting solar evaporation system based on a vertically oriented porous polyacrylonitrile foam, J. Mater. Chem. A. 7 (2019) 14620–14628.
8. Q. Zhang, X. Xiao, G. Wang, X. Ming, X. Liu, H. Wang, H. Yang, W. Xu, X. Wang, Silk-based systems for highly efficient photothermal conversion under one sun: portability, flexibility, and durability, J. Mater. Chem. A. 6 (2018) 17212–17219.
9. W. Huang, G. Hu, C. Tian, X. Wang, J. Tu, Y. Cao, K. Zhang, Nature-inspired salt resistant polypyrrole–wood for highly efficient solar steam generation, Sustain. Energy Fuels. 3 (2019) 3000–3008. https://doi.org/10.1039/C9SE00163H.